THE ASTROPHYSICAL JOURNAL, 237:734–748, 1980 May 1

MOLECULAR CLOUDS ASSOCIATED WITH REFLECTION NEBULAE. I. A SURVEY OF CARBON MONOXIDE EMISSION

MARC L. KUTNER AND DENNIS E. MACHNIK
Physics Department, Rensselaer Polytechnic Institute
KENNETH D. TUCKER
Physics Department, Fordham University
AND
ROBERT L. DICKMAN
The Aerospace Corporation
Received 1979 August 28; accepted 1979 October 31

ABSTRACT

We present 2.6 mm wavelength CO and ^{13}CO observations of 130 molecular clouds associated with reflection nebulae. Enhanced CO emission was found in the vicinity of the illuminating star in about half the objects studied. There is a tendency for the CO peak to be slightly displaced from the star. We find many examples of peaks that appear to result from heating of the cloud by the nearby star, while others appear to be associated with independent concentrations of material.

Subject headings: interstellar: molecules — nebulae: reflection

I. INTRODUCTION

Reflection nebulae mark clear associations between stars and interstellar clouds. The stars illuminating reflection nebulae may have been born close to the sites at which they are currently observed (within the clouds being illuminated) or may be far from their birth sites (merely illuminating the clouds by chance encounter). In either case, molecular observations of the regions around reflection nebulae are of considerable interest. If the illuminating stars were born in the clouds, then star formation in the cloud must have been relatively recent, since the stars have not moved far from their birth sites. This allows a study of conditions in clouds which have recently formed at least one star. Of course, it may be that the star formation process is continuing and that other stars are being formed within the cloud. In this sense, a reflection nebula may serve as a flag, calling our attention to star formation sites within a cloud. An example of such a complex is the strong molecular source associated with the R-association (association of reflection nebulae) Mon R2 (Kutner and Tucker 1975; Beckwith *et al.* 1976; Loren 1977). Sites of multiple star formation provide an excellent opportunity to study the fragmentation of a molecular cloud as the star formation process continues.

Regardless of whether or not a particular star illuminating a reflection nebula was formed in the cloud we now see, the star may have a significant effect on the thermal balance of the cloud. This provides an opportunity to study heating and cooling in a cloud where there is an identifiable dominant energy source (but an energy source that is not as disruptive as one or more O stars, which will give rise to a large H II region). An additional advantage of studying clouds with reflection nebulae is the opportunity to establish a reliable length scale for the clouds. Existing spectroscopic and photometric data for many reflection nebulae are good enough to allow reliable estimates of distances to the stars (e.g., Racine 1968). Since the star and the cloud must be at the same distance, this allows one to convert angular scales for the molecular observations to actual distances. This means that one can estimate cloud masses (e.g., Dickman 1978), as well as the sizes of various substructures within the cloud.

Because of the potential value of studying molecular clouds associated with reflection nebulae, we have made a survey of emission from the $J = 1 \rightarrow 0$ transitions of CO and the isotopically substituted species ^{13}CO, in a number of reflection nebulae. (Note, unless mass numbers are specified, the most abundant isotope of a given element will be assumed.) The reflection nebulae were chosen from the catalog of van den Bergh (1966) and Racine (1968). The present paper describes the general results of the survey, including preliminary maps of some of the most interesting objects. A more detailed analysis of these results will appear elsewhere (Machnik *et al.* 1980*b*; hereafter Paper II).

II. OBSERVATIONS

The observations were carried out on two telescopes, the 11 m telescope of the National Radio Astronomy Observatory[1] on Kitt Peak, and the 4.6 m

[1] The National Radio Astronomy Observatory is operated by Associated Universities Incorporated, under contract with the National Science Foundation.

TABLE 1

OPTICAL PROPERTIES OF STARS ILLUMINATING REFLECTION NEBULAE

VDB	HD/BD	RA(1950)	DEC(1950)	SPT	DIST. MOD	COMMENTS
1A	+57 09	0 6 46	+58 23 16	B5V	8.5	(CAS R1)
1B	+57 18	0 7 59	+58 28 13	B3IV	9.4	(CAS R1)
1C	+57 19	0 8 4	+58 28 5	B6V	8.6	(CAS R1) 9 MIN FROM LK HA 198
2	+64 13	0 10 38	+65 20 4	B2.5V	9.0	(CAS R1)
3	3637	0 31 38	+69 9 33	KOIII	6.3	
4	+61 154	0 40 24	+61 38 42	B EQ		NEAR NGC 225
5	5394	0 53 40	+60 26 47	BOIVE	6.8	IC,59,63 ELEPHANT TRUNKS
6	+61 315	1 40 16	+61 35 0	AOIB	11.3	
7	17138	2 44 23	+69 25 33	A2V	4.5	RZ CAS
8	17443	2 47 9	+67 36 34	B9V	6.6	
9	17463	2 47 29	+68 40 59	F6IB-II	7.4	SU CAS
10	20041	3 11 58	+56 57 22	AOIA	9.8	(CAM R1)
11	20798	3 20 5	+61 21 42	B2III	9.6	(CAM R1)
12	21110	3 22 18	+31 33 21	K4III-IV	6.1	(TAU R2)
13	+30 540	3 22 45	+30 45 26	B8V	7.3	(PER R1)
14	21291	3 25 0	+59 46 5	B9IA	9.4	(CAM R1)
15	21389	3 25 54	+58 42 26	AOIA	10.0	(CAM R1)
16	+29 565	3 25 17	+29 37 36	FOV	5.7	(TAU R2)
17	+30 549	3 26 17	+31 14 10	B8V	8.5	(PER R1) NGC 1333
18	22114	3 31 56	+37 50 57	B8VP	7.3	(PER R1)
19	281159	3 41 26	+32 0 23	B5V	7.4	(PER R1) IC 348
24	275877	3 46 17	+38 49 50	A2II+B6	11.2	XY PER
25	26514	4 9 25	+23 26 51	G6III	5.3	(TAU R2)
26	26676	4 10 50	+10 5 12	B7V	5.5	(TAU R2) H&R 34N
27	283571	4 18 48	+28 19 33	F8E-G2E		RY TAU
28	284419	4 19 3	+19 24 47	KOIIIE		T TAU
29	30378	4 45 13	+29 41 9	B9.5V	5.9	(TAU R2)
30	30614	4 49 4	+66 15 39	O9.5IA	9.5	(CAM R1) ALPHA CAM
31	31293	4 52 34	+30 28 22	AOEP	5.4	(TAU R2) AB AUR, L1517
32	+44 1080	4 58 45	+44 11 54	B5IV	7.4	
34	34078	5 13 0	+34 15 25	O9.5V	7.5	AE AUR
38	34989	5 19 0	+ 8 22 51	B1V	7.5	NEAR S263
39	243202	5 21 12	+32 46 24	B5VP	9.3	
40	243588	5 22 57	+ 6 32 42	G8III	6.9	(TAU-ORI R1)
41	244068	5 26 8	+23 39 40	F4V	6.0	(TAU R2)
43	+5 951	5 29 27	+ 6 0 42	B8V	7.9	(TAU-ORI R1)
44	36540	5 29 46	- 4 33 12	B7III-IV	8.7	(ORI R1/R2)
45	245259	5 33 26	+31 49 54	B8	9.7	
47	37387	5 36 12	+23 17 46	K2IB	9.7	
50	37674	5 37 42	- 1 29 17	B3N	9.5	(ORI R1/R2)
51	37776	5 38 24	- 1 31 55	B2V	9.1	(ORI R1/R2)
53	-10 1261	5 39 2	-10 20 55			
54	-6 1287	5 39 27	- 6 16 39		8.2	(ORI R1/R2) NEAR ORION NEB
55	38023	5 39 57	- 8 9 22	B4V	7.9	
56	38065	5 40 50	+16 20 13	A2V	7.1	
57	38087	5 40 29	- 2 20 5	B3N	8.8	(ORI R1/R2) NEAR NGC 2024
59	38563	5 44 10	+ 0 3 34	B5	8.7	(ORI R1/R2) NGC 2068
63	288309	5 53 42	+ 1 51 32	K		
65	+30 1096	6 1 20	+30 30 46		10.3	
66	-9 1310	6 0 42	- 9 42 10		9.6	(MON R2)
68	42004	6 5 37	- 6 13 8	B1.5V	9.8	(MON R2)-NORTH OF MON R2 MOL PEAK
69	-6 1418	6 5 39	- 6 21 11	B2.5V	9.4	(MON R2)-NEAR MON R2 MOL PEAK
70	42050	6 5 59	- 5 19 51	B1V	9.6	(MOR R2)
71	252680	6 7 11	+14 5 8	B2V	10.1	(MON R1)
72	42261	6 7 49	- 6 18 57	B3V	9.2	(MON R2)-NEAR MON R2 MOL PEAK

TABLE 1—*Continued*

VDB	HD/BD	RA(1950)	DEC(1950)	SPT	DIST. MOD	COMMENTS
74	-6 1444	6 9 23	- 6 8 1	B6	9.6	
75	43836	6 16 20	+23 17 46	B9II	8.7	
76	258686	6 28 1	+10 6 21	B7IIIP	10.1	(MON R1)
77	258749	6 28 9	+ 9 51 27	B5III	10.8	(MON R1)
78	258853	6 28 30	+ 9 49 36	B4NN	9.8	(MON R1)
79	258973	6 28 57	+10 22 34	A2		NEAR MON R1
80A	46060	6 28 27	- 9 37 6	B3N	9.4	(MON R2)
81	46300	6 30 12	+ 7 22 16	A0IB	9.6	(MON R1)
82	259431	6 30 19	+10 21 38	B3PE		NGC 2247
85	289120	6 44 17	+ 1 22 45	B2NE	11.2	NGC 2282
86	51479	6 54 46	-10 12 46	B7V	8.1	(CMA R1)
87A	52329	6 58 5	- 8 47 42	B8	8.5	(CMA R1) ALSO 87B,C
88	52721	6 59 29	-11 13 41	B3E	9.7	(CMA R1)
90A	52942	7 0 22	-11 22 46	B3N	8.6	(CMA R1)
92A	-11 1763	7 1 33	-11 29 59		9.4	(CMA R1) NEAR Z CMA
93	53367	7 2 4	-10 22 44	B0IVE	9.3	(CMA R1) IC 2177
94	53623	7 2 57	-12 14 57	B2V	9.6	(CMA R1) S 297
95	53974	7 4 20	-11 12 57	B0.5IV	9.5	(CMA R1)
96	57281	7 17 32	-23 55 51	B9	10.1	
97	-16 2003	7 30 10	-16 47 18		10.7	
98	61071	7 34 27	-25 13 13	B6V	7.9	
99	143018	15 55 49	-25 58 18	B1V+B2V	5.7	(SCO R1)
100A	145502	16 9 5	-19 19 56	B2IV-V	5.9	(SCO R1)
101	146834	16 16 12	-20 5 51	G5III	4.1	(SCO R1)
102A	147009	16 17 8	-19 55 31	B9.5V	5.5	(SCO R1) ALSO 102B
103A	147103	16 17 35	-19 59 44	A0V	5.6	(SCO R1) ALSO 103B
104	147165	16 18 9	-25 28 28	B1III	5.8	(SCO R1)
105	147889	16 22 23	-24 21 7	B2V	6.1	(SCO R1) RHO OPH MOL SOURCE
106	147933/4	16 22 35	-23 19 58	B2IV+B2V	5.8	(SCO R1) RHO OPH
108	148605	16 27 10	-25 0 24	B2V	5.8	(SCO R1)
110	-20 4896	17 17 8	-20 28 46			
111	156697	17 16 26	+ 6 8 11	FON		
112	-5 4524	17 50 52	- 5 36 42			
113	165784	18 5 39	-21 27 30	A2IA	11.1	(SGR R1)
115	165872	18 6 6	-23 26 40	B3V	9.8	(SGR R1)
116	166288	18 7 42	-17 44 36	B8	8.9	(SGR R1)
118	167638	18 13 54	-19 48 33	B5	10.5	(SGR R1) NEAR NGC 6589
119A	313095	18 14 8	-19 53 55	B5	11.0	(SGR R1) NEAR NGC 6589
120	167746	18 14 23	-16 56 52	G5		
121A	-17 5136	18 17 0	-17 5 43			(SGR R1) SMALL CLUSTER OF NEBULAE
122	-13 4965	18 21 43	-13 41 27	B3N+BO		
123	170634	18 27 52	+ 1 11 17	B7V	8.2	S68
124	170740	18 28 39	-10 49 55	B2V	6.1	
125	182830	19 23 44	+15 27 22	F0		
126	182918	19 24 4	+22 39 23	B6V	8.4	
127	187076/7	19 45 9	+18 24 35	M2II+B6	6.3	
128	190603	20 2 38	+32 4 33	B1.5IA	9.6	(CYG R1)
129	191692	20 8 43	- 0 58 16	B9.5III	3.0	
130A	228789	20 15 53	+39 10 53	B	9.7	(CYG R1)
131	+41 3731	20 22 33	+42 8 15	B3N	10.2	(CYG R1) NGC 6914B
132	+41 3737	20 23 2	+42 13 17	B3VN	10.0	(CYG R1) SAME CLOUD AS NO. 131
133	195593	20 29 5	+36 45 59	F5IAE	10.9	(CYG R1)
134	195556	20 28 31	+48 46 58	B2V	6.8	
135	+31 4152	20 34 45	+32 16 48	M1IIIE	7.7	
136	196819	20 36 30	+41 53 50	K3II	8.0	

TABLE 1—*Continued*

VDB	HD/BD	RA(1950)	DEC(1950)	SPT	DIST. MOD	COMMENTS
137	199478	20 54 8	+47 13 31	B8IA	11.3	
138	199714	20 55 36	+48 6 7	B8IB	12.6	
139	200775	21 1 0	+67 57 56	B5E		
140	203025	21 15 56	+58 24 4	B2IIIE	8.5	
141	+67 1300	21 15 44	+68 3 5			
142	239710	21 35 9	+57 16 38	B3V	9.3	IC 1396 'ELEPHANT TRUNK'
143	206135	21 36 1	+67 57 37	B3V	9.5	(CEP R2)
144	206509	21 39 4	+54 38 39	KOIII	4.1	
145	206887	21 41 46	+48 39 15	F2II-III	7.2	
146A	+65 1637	21 41 40	+65 52 57	B2NNE	12.2	NGC 7129 LK HA 234
147	+46 3471	21 50 38	+46 59 7	B9.5VE	8.2	NEAR IC5146
148	239856	22 5 31	+55 59 21	F2IAB		
150	210806	22 8 50	+73 8 40	B8IV	8.5	(CEP R2)
151	211073	22 11 44	+39 27 58	K3III	3.6	
152	+69 1231	22 12 14	+70 0 11	B9.5V	8.0	(CEP R2)
153	+61 2292	22 21 23	+62 27 36	B2IV-III	8.9	(CEP R1)
154	+64 1677	22 29 35	+65 12 32	B2IV-III	9.7	(CEP R1)
155	216629	22 51 18	+61 52 46	B2PE	8.8	(CEP R1)
157	217903	23 0 36	+72 27 39	B9V	7.1	(CEP R2)
158	222142	23 35 26	+48 13 12	B8V	8.4	

NOTES.—Numbers in column marked "VDB" refer to numbers in catalog of van den Bergh (1966). Spectral type and distance modulus from Racine (1968). Comments in parentheses indicate membership in R-association as identified by van den Bergh (1966).

telescope of the Aerospace Corporation in El Segundo, California.[2] For the CO observations the half-power beamwidth was 1.′1 for the 11 m observations and 2.′6 for the 4.6 m observations. Filter banks provided velocity resolutions of 0.65 km s^{-1} for the Aerospace data and 0.26 km s^{-1} for the NRAO data. For the Aerospace data, frequency switching was employed to achieve acceptable baselines. For the Kitt Peak data, some observations were made with position switching of the telescope every minute, and other observations were made with frequency switching. For the frequency-switched data it was necessary to subtract an off-source spectrum from the on-source spectra. Correction for atmospheric attenuation was carried out as discussed by Kutner (1978), and the peak radiation temperature for CO in the direction of the Kleinmann-Low nebula was 70 K for the NRAO observations and 65 K for the Aerospace observations. A number of sources were observed with both telescopes, and good agreement was found in the overlap regions.

For each reflection nebula, at least five positions were observed in CO—one position in the direction of the star and positions 2′ (or 2.′5) north, south, east and west of the star. Observations of the positions away from the star were made even when no CO was detected in the vicinity of the star. This was done because we found a tendency for the CO emission to peak just off the star, and because exciting stars often lie at the edges of the clouds. In these cases a negative result in the direction of the star could be misleading. In general, when CO was detected at one of the five positions, more extensive mapping was done. However, some of the maps are incomplete in the sense that they do not clearly delineate the peaks in the vicinity of the star. Observations of ^{13}CO were made in sources showing relatively strong CO; typically, ^{13}CO was observed at about half the number of positions which were observed in the common isotopic line.

Optical properties of the stars illuminating the observed reflection nebulae are listed in Table 1. Though several of these nebulae have other designations, it is convenient to refer to all of them by their number in van den Bergh's (1966) catalog. The spectral type and distance modulus data are taken from Racine (1968). Other designations are given in the last column. Comments in parentheses indicate membership in one of the R-associations identified by van den Bergh.

Results of the CO survey are summarized in Table 2. Line parameters are given for the important positions in each source, with offsets in R.A. (seconds of time) and decl. (minutes of arc) listed relative to the coordinates given in Table 1. For each source, the line parameters in the direction of the star are given first, whether or not there is a CO peak in this direction. After that, positions that are CO or ^{13}CO peaks are listed in order of increasing right ascension and declination. Line parameters—peak radiation temperature, LSR velocity of the peak and full line width at half maximum—are given first for CO and then for

[2] The Aerospace spectral-line radio astronomy program was supported jointly by National Science Foundation grant MPS 73-04554 and the Aerospace Corporate Programs for Research and Investigation.

TABLE 2

SUMMARY OF CO OBSERVATIONS

VDB NO.	(ΔRA, ΔDEC) (S, ')	T12 (K)	V(LSR) (KM/S)	DV (KM/S)	T13 (K)	V(LSR) (KM/S)	DV (KM/S)	NOTES
1A	(0.0, 0.0)	<3.0						
1B	(0.0, 0.0)	<3.0						
1C	(0.0, 0.0)	3.0	-11.4	1.5				
2	(0.0, 0.0)	5.6	-19.3	1.5				NOT PEAK
	(-13.0, -1.5)	7.4	-18.0					DV/DR = 3 KM/S/PC N-S
	(-13.0, 2.5)	7.2	-21.0					
3	(0.0, 0.0)	1.8	-6.8	0.8				NOT PEAK
	(-28.0, 0.0)	4.4	-6.8	2.8				INCOMPLETE MAP
4	(0.0, 0.0)	5.2	3.9	3.4				NOT PEAK
5	(0.0, 0.0)	<3.0						
6	(0.0, 0.0)	2.7	-14.2	1.0				NOT PEAK
	(-20.0, 5.0)	7.5	-14.2	1.3				INCOMPLETE MAP
7	(0.0, 0.0)	4.0	-14.0	4.5				NOT PEAK
	(-28.0, 0.0)	6.3	-12.7	2.0				INCOMPLETE MAP
8	(0.0, 0.0)	<2.0						
	(-30.0, 0.0)	3.5	-11.6	0.6				NOT PEAK
9	(0.0, 0.0)	<2.0						
10	(0.0, 0.0)	<3.0						
11	(0.0, 0.0)	<3.0						
12	(0.0, 0.0)	6.7	1.7	2.2	2.2	2.3	1.8	NOT PEAK
	(40.0, 2.5)	9.7	1.1	1.3				MULTIPLE PEAKS & VEL COMPS.
	(60.0, -2.5)	10.4	0.6	2.0				
13	(0.0, 0.0)	8.4	6.6	2.8				PEAK AT ITS VEL
	(48.0, 7.5)	13.4	7.4	1.2				
14	(0.0, 0.0)	1.6	7.6	0.6				NOT PEAK
15	(0.0, 0.0)	<3.0						
16	(0.0, 0.0)	8.2	5.0	2.3				NOT PEAK
	(12.0, 0.0)	10.0	5.6	2.0				EXTENDED REGION OF CONSTANT T12
								DV/DR = 10 KM/S/PC E-W
17	(0.0, 0.0)	28.0	7.2	3.0				FROM LOREN(1975)
18	(0.0, 0.0)	<2.0						
19	(0.0, 0.0)	14.7	8.4	1.8	6.3	8.4	1.4	LOCAL MIN IN T12, (CS,HCN)
	(-68.0, -8.0)	24.0	8.9	1.6	9.0	9.1	1.1	STRONG T13, INCOMPLETE MAP
	(-24.0, -5.0)	25.2	8.3	2.3				
	(0.0, 1.0)	20.1	8.7	1.5	5.6	7.8	1.7	T13 PEAK, (CS,HCN)
	(4.0, 0.0)	20.4	8.7	1.6	4.1	8.3	0.8	PEAK NEAR STAR
24	(0.0, 0.0)	7.5	-4.6	3.5				NOT PEAK
	(-26.0, 0.0)	8.5	-3.2	1.9				INCOMPLETE MAP
25	(0.0, 0.0)	2.8	11.1	0.5				NO MAP
26	(0.0, 0.0)	<2.0						

TABLE 2—*Continued*

VDB NO.	(ΔRA, ΔDEC) (S, ')	T12 (K)	V(LSR) (KM/S)	DV (KM/S)	T13 (K)	V(LSR) (KM/S)	DV (KM/S)	NOTES
27	(0.0, 0.0)	7.0	7.8	1.1	1.2	7.6	1.1	NOT PEAK
	(0.0, 2.5)	10.1	7.7	0.6	2.2	7.6	0.6	LOCAL T12 PEAK
	(11.0, 5.0)	8.4	7.9	0.8	3.3	8.1	0.5	T13 PEAK
	(22.0, 2.5)	10.9	7.8	0.6	1.6	8.1	0.4	
28	(0.0, 0.0)	3.0	6.3	1.0				NOT PEAK
29	(0.0, 0.0)	5.6	7.0	1.5	1.1	7.5	1.3	NOT PEAK (CLOUD EDGE)
	(-48.0,-10.0)	10.3	6.7	2.0	2.6	5.6	1.4	DV/DR = 9 KM/S/PC
	(-24.0, -5.0)	10.9	5.4	1.0	2.0	5.6	1.0	EXTENDED REGION WITH T12=10 K
30	(0.0, 0.0)	<3.0						
31	(0.0, 0.0)	12.1	6.8	0.6	1.6	6.6	0.8	SEE ALSO LOREN(1975)
	(-24.0, 0.0)	7.7	6.0					SUB-PEAK AT 6 KM/S
	(0.0, -5.0)	7.6	6.0					SUB-PEAK AT 6 KM/S
	(12.0, 0.0)	6.8	6.0					SUB-PEAK AT 6 KM/S
32	(0.0, 0.0)	4.4	-2.4	5.2				NOT PEAK
34	(0.0, 0.0)	2.5	6.8	0.5				NOT PEAK
38	(0.0, 0.0)	3.0	0.7	0.8				NOT PEAK
	(-40.0, -2.5)	13.3	0.2	0.9	3.1	0.3	0.6	S263
39	(0.0, 0.0)	2.6	7.4	0.6				NOT PEAK
40	(0.0, 0.0)	3.2	-5.4	0.6				NOT PEAK
41	(0.0, 0.0)	7.5	7.8	1.3	1.0	8.2		NOT PEAK
	(36.0, -7.5)	11.0	7.6	1.6	2.3	8.1	0.8	EXTENDED 11 K T12
43	(0.0, 0.0)	7.3	-10.3	0.7				
44	(0.0, 0.0)	2.3	11.0	3.9				NOT PEAK
	(-40.0, 0.0)	13.7	11.1	2.9				INCOMPLETE MAP
45	(0.0, 0.0)	13.1	-17.0	2.8	3.1	-18.0	1.4	PEAK AT ITS VEL
	(-12.0, -2.5)	17.1	-18.8	3.0	4.1	-18.6	2.4	
47	(0.0, 0.0)	4.3	2.3	2.7				NOT PEAK
		3.3	5.6	1.6				
	(-55.0,-17.5)	7.8	1.2	2.2				INCOMPLETE MAP - LONG RIDGE, DV/DR = 0.5 KM/S/PC
50	(0.0, 0.0)	4.8	2.1	0.5				NOT PEAK
51	(0.0, 0.0)	13.2	9.9	2.3	1.5	9.7	0.7	NEAR NGC 2024
		10.0	11.2	1.1	1.3	11.3	0.8	
	(4.0, -1.0)	16.9	9.3	2.6				PROBABLY ASSOC. WITH R-NEB
		13.1	11.2	1.0	3.0	11.0	0.8	
	(12.0, -1.0)	18.9	8.4	3.0	5.1	8.5	0.8	MAY BE ASSOC. WITH 2024
		16.6	9.6	3.0				
	(16.0, 0.0)	17.4	9.1	2.6	6.3	8.8	1.1	MAY BE ASSOC. WITH 2024 (CS,HCN)
53	(0.0, 0.0)	3.0	2.6	1.0				NO PEAK
54	(0.0, 0.0)	18.8	7.7	1.2				DV/DR = 1.6 KM/S/PC
55	(0.0, 0.0)	26.4	2.9	1.5				
	(10.0, -2.5)	29.3	2.4	1.4				
56	(0.0, 0.0)	1.9	8.9	0.8				NOT PEAK
57	(0.0, 0.0)	3.6	9.5	1.8				NOT PEAK
	(0.0, 5.0)	15.6	10.0	2.9				T12 STRONG TO NORTH

TABLE 2—*Continued*

VDB NO.	(ΔRA, ΔDEC) (S, ')	T12 (K)	V(LSR) (KM/S)	DV (KM/S)	T13 (K)	V(LSR) (KM/S)	DV (KM/S)	NOTES
59	(0.0, 0.0)	37.0	0.0		10.0	0.0		(CS), SEE ALSO KTT
63	(0.0, 0.0)	2.5	12.0	0.1				NOT PEAK
65	(-1.0, -0.5)	4.8	3.0	2.1				NOT PEAK
	(11.0, -0.5)	10.5	3.0	1.9				DV/DR = 1.5 KM/S/PC
66	(1.0, 1.0)	14.9	13.9	0.5	3.3	13.0	0.5	PEAK ON 14 KM/S MAP
	(11.0, 1.5)	16.9	12.5	1.8	6.4	13.0	2.3	
68	(0.0, 0.0)	5.0	10.5	2.0	1.4	10.6	0.5	NOT PEAK
	(0.0, -4.0)	14.7	9.5	1.5	5.1	9.5	1.3	CONFUSED WITH MON R2 EMISSION
69	(0.0, 0.0)	21.6	9.9	2.3	1.0	11.8	1.5	CONFUSED WITH MON R2 EMISSION
70	(0.0, 0.0)	<3.0						
71	(0.0, 0.0)	<3.0						
72	(0.0, 0.0)	4.2	8.4	0.5	2.1	6.4	0.5	NOT PEAK
	(-8.0, -2.0)	11.1	8.9	1.4	3.2	8.6	0.8	MAY BE ASSOC. WITH NGC 2183
74	(-3.0, 0.0)	11.6	11.4	1.2	3.8	11.3	1.1	
75	(0.0, 0.0)	2.2	3.0	0.8				NOT PEAK
76	(0.0, 0.0)	2.3	-1.0	1.3				NOT PEAK
	(-20.0, -2.5)	14.3	-0.4	2.4				EXTENDED HIGH T12 REGION (SEE KDTM)
77	(0.0, 0.0)	17.0	-0.3	1.0	1.9	-0.1	1.0	EXTENDED HIGH T12 REGION (SEE KDTM)
	(-20.0, 6.0)	18.4	-0.2	1.5	1.4	0.1	0.5	
	(4.0, 0.0)	17.9	-0.4	1.1	3.3	-0.1	1.1	
78	(0.0, 0.0)	4.0	1.2	0.8				NOT PEAK
	(20.0, 2.5)	12.1	1.1	0.7				
79	(0.0, 0.0)	1.7	0.1	0.8				NOT PEAK
	(-36.0, 5.0)	13.3	-1.2	1.9				ASSOC. WITH IC446 (AFCRL 951)
80A	(0.0, 0.0)	3.9	12.3	1.0	1.9	11.5	0.8	NOT PEAK
	(-4.0, 4.0)	15.2	12.9	1.5	4.0	12.8	1.3	
81	(0.0, 0.0)	<2.0						
82	(0.0, 0.0)	17.6	4.8	1.7	3.9	5.0	0.8	NEAR MON R1 (SEE ALSO KDTM,LOREN 1976)
85	(0.0, 0.0)	12.2	22.0	1.3	1.2	23.7	0.6	NOT PEAK
	(10.0, -2.5)	11.4	21.1	2.0	1.9	21.9	0.8	
	(10.0, 0.0)	15.8	21.2	1.9	2.7	22.0	0.8	T12 AND T13 PEAK
86	(0.0, 0.0)	4.6	11.5	1.5				NOT PEAK
	(-8.0, 0.0)	7.6	12.3	0.8				INCOMPLETE MAP
87A	(0.0, 0.0)	9.8	40.2	1.8				NOT PEAK
	(0.0, 2.5)	14.4	38.9	2.6				DV/DR = 0.7 KM/S/PC N-S
88	(0.0, 0.0)	3.2	12.7	1.0				LIMITED MAP
90A	(0.0, 0.0)	2.4	14.1	0.5				LIMITED MAP
92A	(0.0, 0.0)	19.8	13.4	1.7	2.6	12.9	0.7	
	(8.0, -1.0)	17.8	13.1	1.3	7.6	12.9	0.5	T13 PEAK AND SECONDARY T12 PEAK DV/DR = 1.8 KM/S/PC (CS,HCN)
93	(0.0, 0.0)	15.4	17.9	3.5	4.4	17.9	2.3	DATA FROM LOREN(1975)

TABLE 2—*Continued*

VDB NO.	(ΔRA, ΔDEC) (S, ')	T12 (K)	V(LSR) (KM/S)	DV (KM/S)	T13 (K)	V(LSR) (KM/S)	DV (KM/S)	NOTES
94	(0.0, 0.0)	2.5	12.1	1.0				NOT PEAK
	(-8.0, 0.0)	14.9	12.6	1.8	2.8	12.4	1.0	T12 PEAK, T13 GETS STRONGER TO NW SEE ALSO BLAIR ET AL.
95	(0.0, 0.0)	4.0	15.6	1.5	<1.0			STAR AT LOCAL T12 MIN
	(20.0, -2.5)	15.6	15.6	3.2	5.3	15.7	2.8	T12 AND T13 PEAK, DV/DR = 0.4 KM/S/PC NE-SW
96	(0.0, 0.0)	<3.0						
	(0.0, -2.5)	4.0	19.6	2.0				INCOMPLETE MAP
97	(0.0, 0.0)	4.2	17.5	1.4	1.8	17.7	0.7	NOT PEAK
	(-10.0, -5.0)	16.5	16.8	2.2	4.0	17.0	1.4	
98	(0.0, 0.0)	<3.0						
	(0.0, 2.5)	3.0	23.0	1.2				INCOMPLETE MAP
99	(0.0, 0.0)	<4.0						
100A	(0.0, 0.0)	2.3	5.1	0.9				NOT PEAK
101	(0.0, 0.0)	<4.0						
102A	(0.0, 0.0)	11.0	3.3	0.7	2.4	3.6	0.7	NOT PEAK
	(12.0, 2.0)	16.6	3.3	0.8	1.8	3.7	0.5	
103A	(0.0, 0.0)	10.5	3.3	1.3	2.5	3.4	0.8	NOT PEAK
	(22.0, 0.0)	19.0	3.3	1.2	6.5	3.2	0.8	T13 PEAK
	(33.0,-10.0)	22.4	3.3	1.8	3.4	3.3	0.9	EXTENDED PEAK
	(33.0, 5.0)	25.0	3.0	1.3	4.2	3.2	0.8	EXTENDED PEAK
104	(0.0, 0.0)	<3.0						
105	(0.0, 0.0)	22.7	3.6	1.3				NOT PEAK
	(11.0, 0.0)	30.9	3.6	1.4				INCOMPLETE MAP (SEE ENCRENAZ)
106	(0.0, 0.0)	<4.0						
	(0.0, 2.0)	4.8	2.3	1.3				INCOMPLETE MAP
108	(0.0, 0.0)	2.0	4.5	0.4				NOT PEAK
110	(0.0, 0.0)	<4.0						
111	(0.0, 0.0)	<3.0						
112	(0.0, 0.0)	7.4	7.1	1.3				
113	(0.0, 0.0)	5.1	23.3	5.5				NOT PEAK
	(0.0, -1.0)	6.4	23.3	2.1				
115	(0.0, 0.0)	16.3	8.7	1.9	5.3	5.1	0.6	STAR AT EDGE OF STRONG T12
	(8.0, -1.0)	20.7	9.2	1.9				T12 PEAK
	(24.0, -2.0)	14.3	8.9	2.5	7.2	9.1	1.3	T13 PEAK AND SECONDARY T12 PEAK (CS,HCN)
116	(0.0, 0.0)	12.7	18.6	2.4	3.7	18.8	2.0	NOT PEAK, 1 DEG FROM W33 BUT DIF. VEL
	(5.0, -2.0)	17.8	19.6	3.1				OTHER PEAKS MAY BE PRESENT
118	(0.0, -0.5)	10.0	12.2	3.0				NOT PEAK
	(8.0, 0.0)	31.7	11.8	3.0	12.8	11.4	2.1	(CS,HCN)
119A	(-2.0, 0.5)	17.5	9.7	1.6	8.4	9.0	4.0	NOT PEAK
	(-10.0, 0.8)	19.9	10.2	4.0	9.3	9.5	2.7	(CS,HCN) SEE ALSO BLAIR ET AL.
120	(0.0, 0.0)	15.0	21.6	2.6	3.7	20.5	2.2	1 DEG FROM M17
	(0.0, -5.0)	15.7	20.3	4.0	5.7	20.8	4.4	

TABLE 2—*Continued*

VDB NO.	(ΔRA, ΔDEC) (S, ')	T12 (K)	V(LSR) (KM/S)	DV (KM/S)	T13 (K)	V(LSR) (KM/S)	DV (KM/S)	NOTES
121A	(0.0, 0.0)	3.1	1.4	1.1				NOT PEAK
122	(0.0, 0.0)	<3.0						
123	(0.0, 0.0)	17.0	7.2	1.5	4.8	7.2	1.1	DISTINCT FROM S68 PEAK OF BLAIR ET AL. AT (-24S,+40'),(CS,HCN)
124	(0.0, 0.0)	3.8	6.9	3.3				NOT PEAK
	(10.0, 0.0)	5.9	6.8	2.2				LIMITED MAP
125	(0.0, 0.0)	<3.0						
126	(0.0, 0.0)	8.1	11.6	2.8	1.2	11.9	2.2	NOT PEAK
	(33.0, -2.5)	13.1	11.8	2.1	3.7	11.9	1.3	
127	(0.0, 0.0)	<3.0						
128	(0.0, 0.0)	<3.0						
	(0.0, 2.5)	3.0	-2.2	0.9				LIMITED MAP
129	(0.0, 0.0)	<3.0						
	(0.0, 2.5)	2.5	0.1	0.8				LIMITED MAP
130A	(0.0, 0.0)	11.3	0.3	3.0	1.9	0.4	1.0	NOT PEAK
	(-12.0, 1.0)	19.4	0.8	3.0	6.3	0.7	1.1	T13 PEAK
	(-8.0, 1.0)	22.4	0.8	2.2	4.7	0.7	1.1	EXTENDED T12 PEAK, DV/DR = 0.8 KM/S/PC
	(0.0, 1.0)	21.6	0.3	2.7	5.7	0.4	1.0	(CS,HCN)
131	(0.0, 0.0)	16.8	4.8	3.1	6.3	5.0	2.0	NOT PEAK (CS,HCN)
	(-6.0, -2.0)	18.6	5.3	3.2	5.0	5.0	1.0	SECONDARY T12 PEAK
	(0.0, -2.0)	15.9	4.8	3.8	7.3	5.0	2.0	T13 PEAK
	(6.0, -2.0)	19.7	5.0	3.3	5.5	5.0	0.9	(CS,HCN) SEE ALSO LOREN 1975
132	(0.0, 0.0)	17.9	5.1	3.0	2.4	4.8	1.1	NOT PEAK-PEAK CURVES AROUND STAR
	(-11.0, 0.0)	24.4	5.0	1.8	6.5	5.0	1.2	T13 PEAK
	(-6.0, 0.0)	31.8	4.8	1.7	4.1	4.8	1.1	SEE ALSO LOREN 1975
	(6.0, 0.0)	22.9	4.7	0.8	1.8	2.5	4.7	
133	(0.0, 0.0)	1.6	-0.4	1.0				NOT PEAK
	(-12.0, 4.0)	9.5	0.1	1.9				
134	(0.0, 0.0)	<3.0						
135	(0.0, 0.0)	4.1	12.4	1.0				NOT PEAK
	(-12.0, -2.5)	5.0	12.4	2.1				LIMITED MAP
136	(0.0, 0.0)	18.5	7.5	1.8	1.4	8.1	0.8	NOT PEAK
	(6.0, 0.0)	26.0	7.9	2.6	4.1	7.6	1.9	DR 21 20' AWAY BUT DIF. VLSR
	(78.0, 2.5)	12.6	10.3	2.0				SUB-PEAK
137	(0.0, 0.0)	2.0	-16.5	1.4				NOT PEAK
138	(0.0, 0.0)	2.0	2.9	0.6				NOT PEAK
139	(0.0, 0.0)	12.0	2.0	3.3	1.7	1.7	1.1	SUB-PEAK
	(44.0, 3.0)	16.7	3.5	3.9	4.2	3.9	1.0	EXTENDED PEAK
140	(0.0, 0.0)	<3.0						
141	(17.0, 0.0)	2.1	3.6	0.8				NO PEAK, LIMITED MAP
142	(0.0, 0.0)	16.5	-8.3	1.9	2.2	-8.3	0.6	
					3.6	-7.5	0.8	NOT PEAK
	(8.0, 0.0)	20.4	-8.3	1.8	4.5	-7.7	0.9	(CS,HCN) SEE ALSO LOREN ET AL. 1975
	(24.0, 0.0)	18.3	-8.0	2.8	6.3	-7.8	1.5	T13 PEAK & T12 SUB-PEAK

TABLE 2—*Continued*

VDB NO.	(ΔRA, ΔDEC) (S, ')	T12 (K)	V(LSR) (KM/S)	DV (KM/S)	T13 (K)	V(LSR) (KM/S)	DV (KM/S)	NOTES
143	(0.0, 0.0)	<3.0						
144	(0.0, 0.0)	5.3	1.1	2.2				NOT PEAK
	(-17.0, 2.5)	8.2	1.3	1.9				EXTENDED RIDGE AT THIS T12
145	(0.0, 0.0)	3.4	20.9	0.8				
146A	(0.0, 0.0)	7.8	-10.6	0.8	2.1	-10.2	0.8	NOT PEAK
	(8.0, 2.0)	18.2	-10.3	2.6	5.0	-10.2	1.3	T12 PEAK (SEE ALSO LOREN 1975)
	(24.0, -1.0)	18.0	-10.3	2.6	7.4	-10.2	1.4	T13 PEAK, T12 SUB-PEAK,(CS,HCN)
147	(0.0, 0.0)	8.5	6.7	1.0	1.6	6.4	0.3	NOT PEAK, STAR AT EDGE OF CLOUD
	(12.0, 1.0)	14.3	6.6	1.5	4.7	6.4	0.7	NEAR IC 5146
148	(0.0, 0.0)	1.8	-1.1	0.8				NOT PEAK, LIMITED MAP
150	(0.0, 0.0)	3.6	-4.1	1.5				NOT PEAK
	(0.0, -2.0)	6.8	-3.9	1.7				LIMITED MAP
151	(0.0, 2.5)	2.6	-12.4	0.5				NO MAP
152	(0.0, 0.0)	10.5	-5.3	1.3	5.1	-5.2	0.9	
153	(0.0, 0.0)	<4.0						
154	(0.0, 0.0)	<3.0						
155	(0.0, 0.0)	4.7	-9.6	1.0	1.1	-10.5	0.5	NOT PEAK, STAR AT EDGE
	(-24.0, 0.0)	22.9	-9.1	2.0	6.4	-9.2	1.0	T12 SUB-PEAK (CS,HCN)
	(-16.0, 3.0)	24.0	-9.6	1.1	6.3	-9.2	1.1	EXTENDED T12 PEAK, T13 PEAK (CS,HCN)
	(16.0, 4.0)	19.3	-9.6	1.5				
157	(0.0, 0.0)	<3.0						
158	(0.0, 0.0)	6.0	-7.9	1.0	<1.0			NOT PEAK
	(-60.0, -5.0)	10.3	-8.2	1.3	4.5	-7.9	0.9	T13 PEAK
	(-48.0, -5.0)	13.7	-8.2	1.3	3.7	-7.9	0.8	EXTENDED T12 PEAK

NOTES.—Offsets are in seconds of time (R.A.) and minutes of arc (decl.) from the coordinates given in Table 1. Line parameters (peak line radiation temperature, LSR velocity of the peak, and full width at half-maximum, DV) are given first for CO and then for ^{13}CO. No entry in the ^{13}CO columns means that no observations of that species were made. Typical rms noise levels were 0.5–1.0 K for CO and 0.3 K for ^{13}CO. In addition we estimate 20% uncertainties in absolute calibration. Upper limits correspond to the peak-to-peak noise level. DV/DR in "NOTES" column refers to observed velocity gradients, converted to km s^{-1} pc^{-1} assuming the distance modulus from Table 1. The direction given (e.g., E-W) is the direction of the gradient and is perpendicular to the projected axis of rotation, if the gradient is due to rotation. The listing of other molecules (e.g., CS, HCN) in the "NOTES" column indicates a detection of those molecules at those positions.

^{13}CO. Additional notes are given in the last column. In some cases, our data duplicate or supplement that of other observers, as indicated in the last column. Also, at some of the positions of strongest ^{13}CO emission, observations of other molecules, such as HCN and CS, were made. These observations are highly incomplete, but the detection of lines from other molecules is noted by listing the appropriate species in the last column of Table 2. Finally, a number of sources show clear velocity gradients in the CO lines, and these are also noted in the last column as "DV/DR =." When a direction is given for such a gradient, it is the direction of maximum velocity increase or decrease and would correspond to a direction perpendicular to the axis of rotation, if the gradient is caused by rotation.

Radiation temperature contour maps of the more extensively sampled regions are presented in Figure 1. Sources for which both CO and ^{13}CO data are available are shown first; those sources for which only CO data is available then follow. Previously published

FIG. 1 (*overleaf*).—Maps of CO and ^{13}CO emission from molecular clouds associated with reflection nebulae. Contours are of peak line radiation temperature. The positions of stars illuminating reflection nebulae are indicated by asterisks (*). The maps are arranged by number in the catalog of van den Bergh (1966), with sources for which there is CO and ^{13}CO data presented first and sources for which there is only CO data at the end. The figures are drawn to different scales, so each map has a line marking 5′ on the sky. In addition, the length scale, assuming the distance modulus given in Table 1, is given by the 1 pc line. In sources with more than one reflection nebula (e.g., 102, 103) the lower number nebula is at lower R.A. (*on the right*).

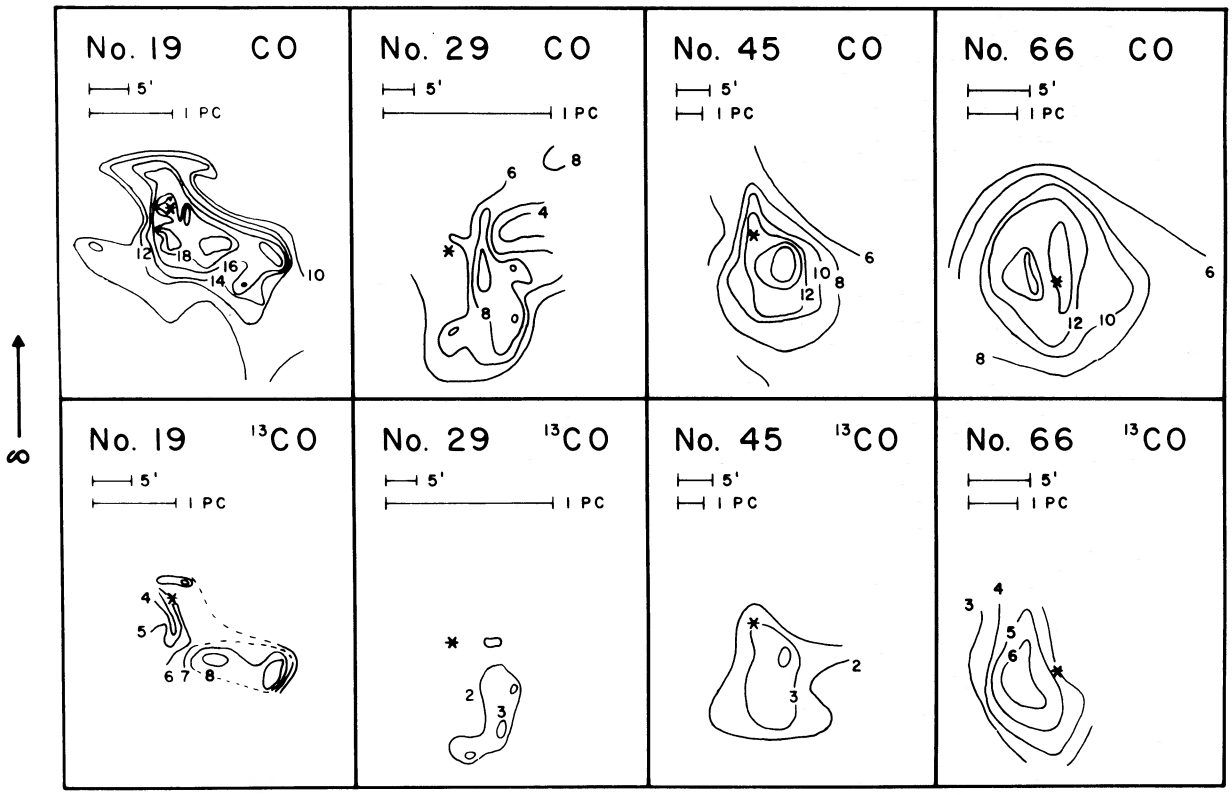

FIG. 1*a*

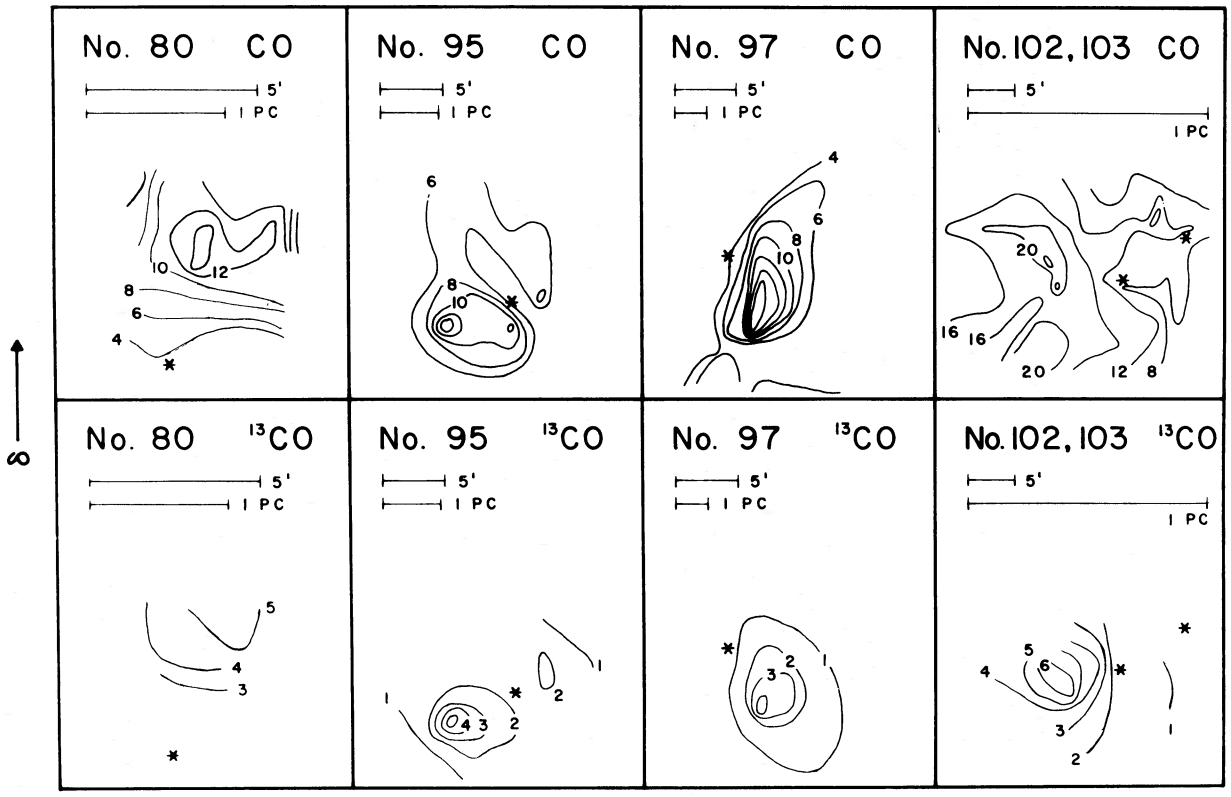

FIG. 1*b*

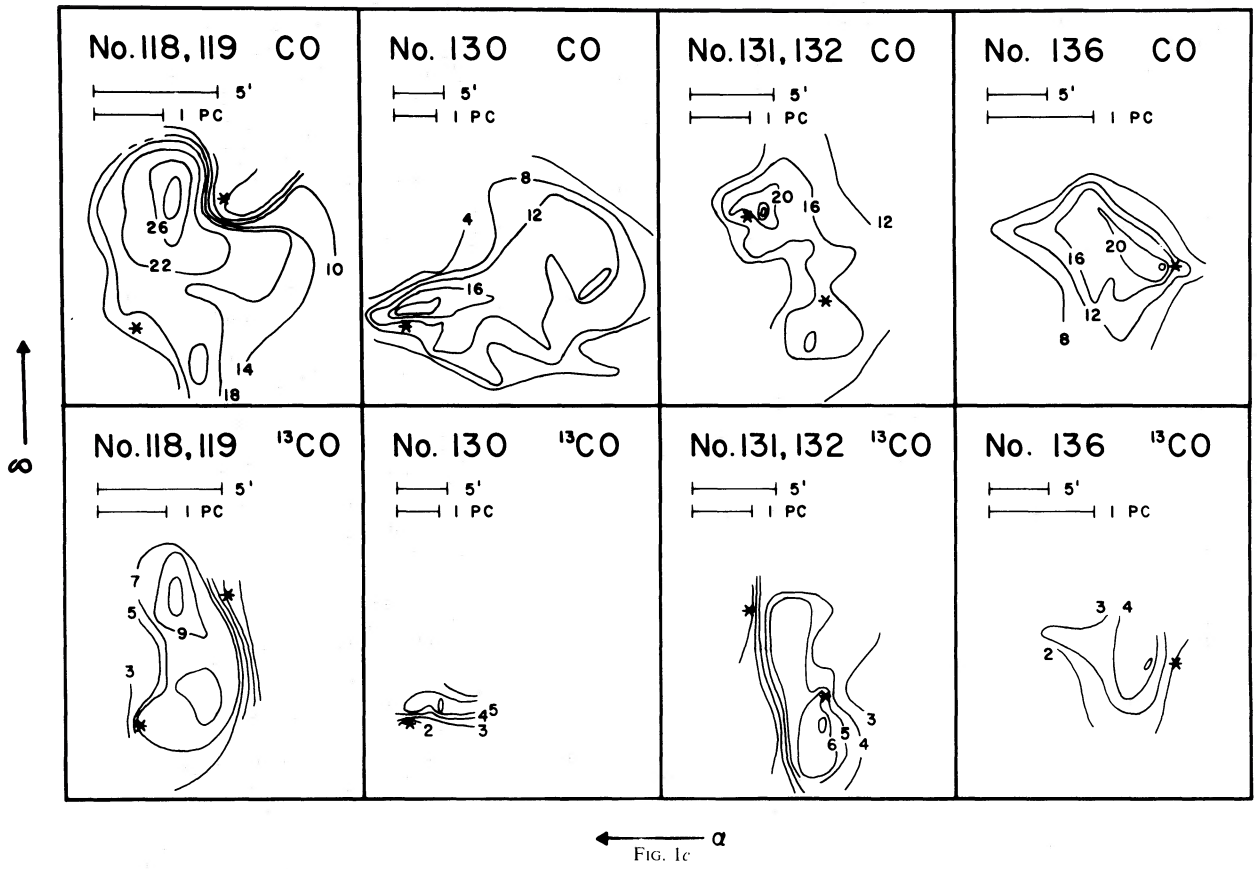

FIG. 1c

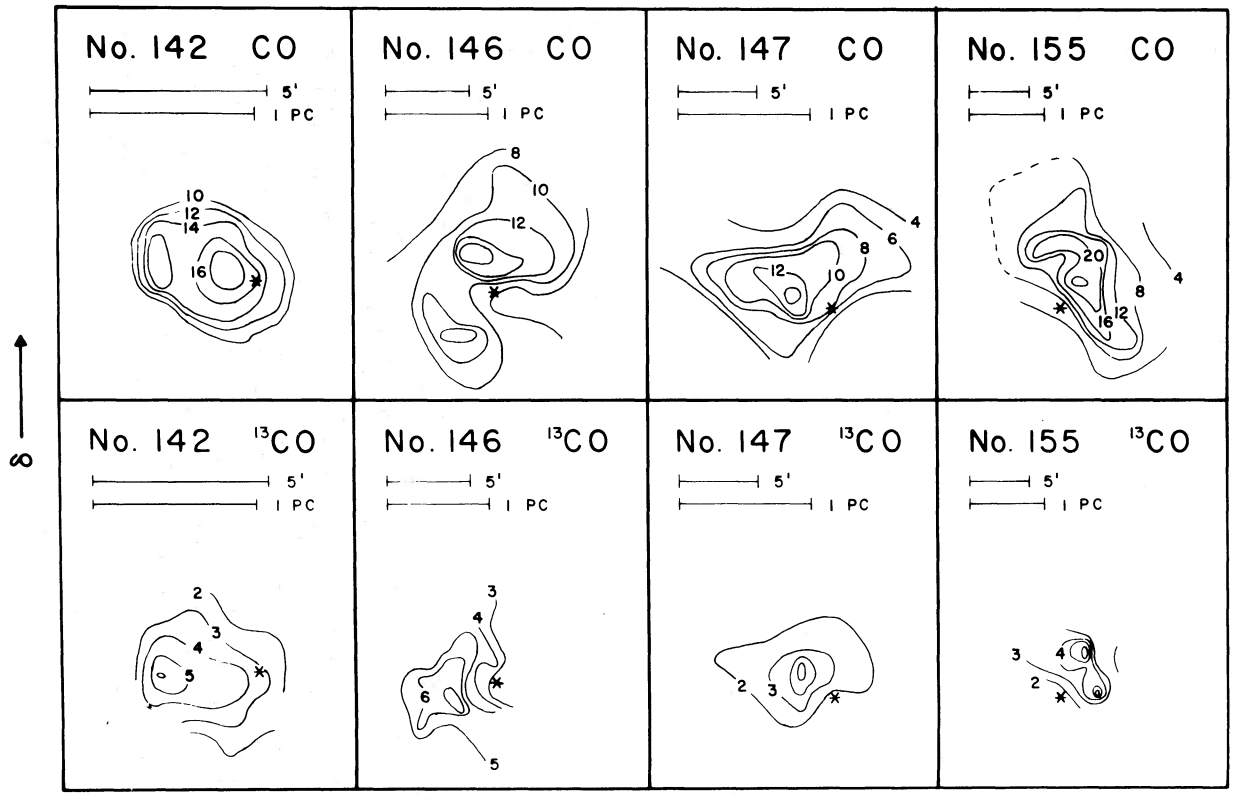

FIG. 1d

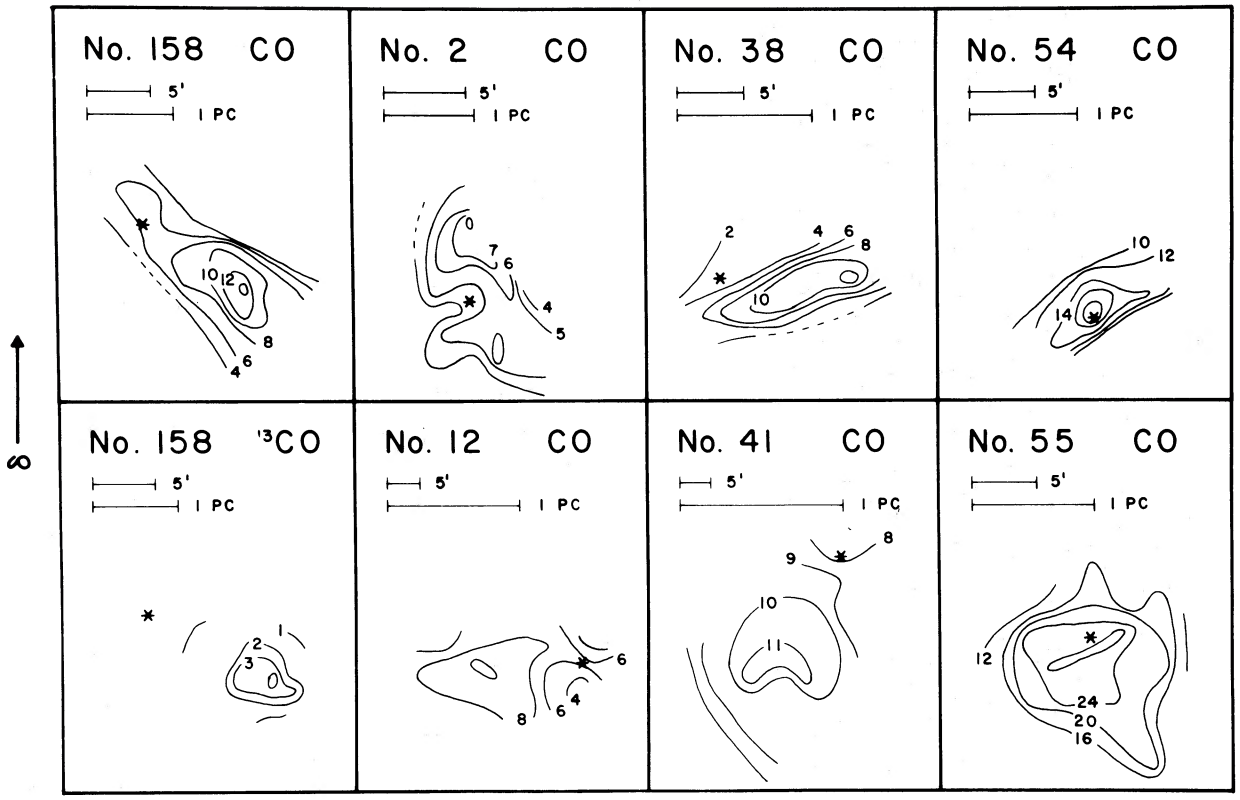

FIG. 1e

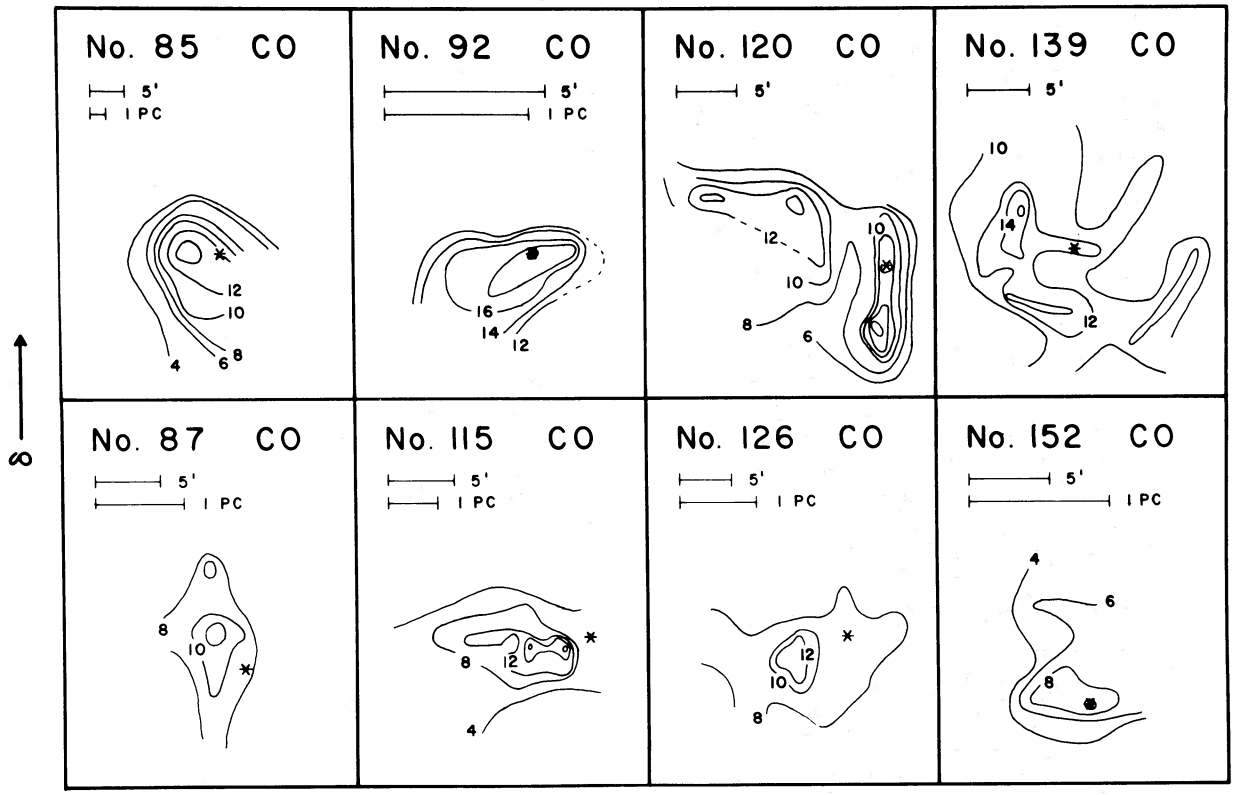

FIG. 1f

CO maps for two R-associations—Mon R1 (Kutner *et al.* 1979) and Mon R2 (Kutner and Tucker 1975)—are omitted. In addition, a more extensive map of the Canis Major R1 region will be published separately (Machnik *et al.* 1980*a*). We note that some of the molecular clouds associated with reflection nebulae have been observed by other workers in other contexts. (We note also that some of the objects also appear in the more limited survey of Knapp *et al.* 1977.) References to these works, which usually include maps of the regions, are given in the last column of Table 2.

III. DISCUSSION

Though the detailed results of the survey will be interpreted in Paper II, we point out here some of the general features that have emerged. Of the 130 objects included in the survey, some indication of enhanced CO emission in the vicinity of the star was found in 62 (48%), and no CO emission at all was found in the vicinity of 28 (21%). In the remaining 40 (31%) only a normal dark cloud CO line was detected. This last number may represent a slight overestimate due to incomplete mapping.

One obvious feature that emerges from inspection of Table 2 and Figure 1 is that even CO peaks that appear most closely associated with illuminating stars do not appear exactly coincident with those stars, often being separated by a few minutes of arc. Moreover, there are numerous cases in which the nebular star appears just at the edge of a region of strong or moderately strong CO emission. Some examples shown in Figure 1 are numbers 29, 80, 95, 97, 102, 118, 130, 132, 136, 146, 147, 155, 2, 38, 41, and 115. An inspection of the Palomar Sky Survey prints indicates that the illuminating stars for most of these appear just to one side of a dark cloud, with the optical nebula often showing the same asymmetry as the CO emission. That is, the optical nebula is visibly more extended on the side of the star that contains the strong CO emission. The fact that this occurs so often in our sample may be just a selection effect, by which the relatively unobscured stars at cloud edges produce more pronounced reflection nebulae than stars embedded within the cloud.

The placement of the star near the edge of a cloud may explain why the CO peaks often appear slightly separated from the star even when the star does not appear clearly beyond the edge of the cloud. If we assume that a CO peak is due to the heating of the cloud near the star, and the star is slightly outside the cloud, the heating will be greatest at the point of the surface closest to the star—the substellar point. For a viewer whose line of sight is perpendicular to the cloud surface, the star appears projected against the CO peak. For any other viewing angle the star appears displaced from the CO peak. This point will be treated in a statistical way in Paper II.

It is clearly of interest to separate those CO peaks that result from simple heating of the cloud by the star from those that result from a density enhancement as well as an increase in cloud temperature. Observations of millimeter emission from rarer molecules, such as HCN or H_2CO, would be the best indicators of density enhancement, but the CO and ^{13}CO data provide the basis for at least a preliminary division. If the CO peak is due to heating of the cloud, with no increase in local gas density or CO column density (which would generally accompany an increase in local density), one would expect little or no enhancement in ^{13}CO emission. There are two reasons for this: (1) If densities are not very high, the excitation temperature of ^{13}CO will be well below the kinetic temperature of the gas, while the excitation temperature of CO will be close to the kinetic temperature because of the effects of radiation trapping in the optically thick CO lines. Therefore, if the kinetic temperature rises, one would expect the CO excitation temperature to increase by more than the ^{13}CO excitation temperature. (2) An increase in the excitation temperature of either species will result in an increase in the population in higher energy levels, decreasing the optical depth in the $1 \rightarrow 0$ transition. For the optically thick CO this has a negligible effect on the line strength, but for ^{13}CO it would serve to minimize any enhancement due to the increase in excitation temperature.

Therefore, as a preliminary classification, we shall refer to peaks in the CO emission without corresponding ^{13}CO peaks as "heating peaks" and peaks in the CO emission with corresponding ^{13}CO peaks as "density peaks." As mentioned, some preliminary observations of HCN and CS in some of the sources have already been made on the 11 m telescope. These were made in the directions of peaks that would be classified as "density" peaks by the above criteria and yielded lines with strengths comparable to those in other sources that have been studied more extensively and found to have higher densities ($n_{H_2} \geq 10^4$ cm^{-3}) than typical dark molecular clouds.

In Figure 1, one finds examples of both types of peaks, with some sources showing both types within the same cloud (e.g., numbers 66, 142, 146, and 158). Of course, more detailed observations of other molecules will be necessary to clearly establish the nature of these peaks. However, it should be noted that the "density" peaks may well mark regions where other stars are being formed within the clouds and might be useful locations for future infrared observations.

More information on the possibility of density enhancements may come from the velocity structure of the cloud. For example, a rotating cloud that has fragmented might show a few peaks at different velocities. Several sources have this type of structure, often with some peaks hidden on peak brightness temperature maps, such as in Figure 1. These peaks show up on maps of emission in a small velocity range. Sources with such structure or with definite velocity gradients are noted in Table 2, and more detailed velocity structure maps will be given in Paper II. Further information on the density/velocity structure of sources will have to come from high-resolution observations of rarer molecules, but such sources may

provide us with an excellent opportunity to study the fragmentation of a cloud in a star forming region.

M. L. K. acknowledges partial support from the National Science Foundation grant AST76-17834 and a grant from the Research Corporation. K. D. T. acknowledges support of a grant from the Research Corporation and from a Fordham University faculty research grant. We also wish to acknowledge the assistance of Messrs. David Leisawitz and Michael Hettrick, who were supported by the National Science Foundation grant SM176-83582 (Undergraduate Research Participation) and Mr. Michael Krikorian, for assistance in the data reduction. We also thank the technical editors of the RPI Office of Computer Services for their help in preparing the tables.

REFERENCES

Beckwith, S., Evans, N. J., II, Becklin, E. E., and Neugebauer, G. 1976, *Ap. J.*, **208**, 390.
Blair, G. N., Peters, W. L., and Vanden Bout, P. A. 1975, *Ap. J. (Letters)*, **200**, L161.
Dickman, R. L. 1978, *Ap. J. Suppl.*, **37**, 407.
Encrenaz, P. 1974, *Ap. J. (Letters)*, **189**, L135.
Knapp, G. R., Kuiper, T. B. H., Knapp, S. L., and Brown, R. L. 1977, *Ap. J.*, **214**, 78.
Kutner, M. L. 1978, *Ap. Letters*, **19**, 81.
Kutner, M. L., Dickman, R. L., Tucker, K. D., and Machnik, D. E. 1979, *Ap. J.*, **232**, 724.
Kutner, M. L., and Tucker, K. D. 1975, *Ap. J.*, **199**, 79.
Kutner, M. L., Tucker, K. D., and Thaddeus, P. 1973, *Ap. J. (Letters)*, **186**, L13.
Loren, R. 1975, Ph.D. thesis, University of Texas, Austin.
———. 1977, *Ap. J.*, **215**, 129.
Loren, R., Peters, W., and Vanden Bout, P. 1975, *Ap. J.*, **195**, 75.
Machnik, D. E., Hettrick, M., Kutner, M. L., Tucker, K. D., and Dickman, R. L. 1980*a*, in preparation.
Machnik, D. E., Kutner, M. L., Tucker, K. D., and Dickman, R. L. 1980*b*, in preparation.
Racine, R. 1968, *A.J.*, **73**, 223.
van den Bergh, S. 1966, *A.J.*, **71**, 990.

R. L. DICKMAN: 130–422, The Aerospace Corporation, P.O. Box 92957, Los Angeles, CA 90009
M. L. KUTNER and D. E. MACHNIK: Physics Department, Rensselaer Polytechnic Institute, Troy, NY 12181
K. D. TUCKER: Physics Department, Fordham University, Bronx, NY 10458